Research Article **Open Access**

Fumiki Sekiya* and Akihiro Sugimoto

On properties of analytical approximation for discretizing 2D curves and 3D surfaces

https://doi.org/10.1515/mathm-2017-0002
Received May 12, 2017; accepted October 17, 2017

Abstract: The morphological discretization is most commonly used for curve and surface discretization, which has been well studied and known to have some important properties, such as preservation of topological properties (e.g., connectivity) of an original curve or surface. To reduce its high computational cost, on the other hand, an approximation of the morphological discretization, called the analytical approximation, was introduced. In this paper, we study the properties of the analytical approximation focusing on discretization of 2D curves and 3D surfaces in the form of $y = f(x)$ $(x, y \in \mathbb{R})$ and $z = f(x, y)$ $(x, y, z \in \mathbb{R})$. We employ as a structuring element for the morphological discretization, the adjacency norm ball and use only its vertices for the analytical approximation. We show that the discretization of any curve/surface by the analytical approximation can be seen as the morphological discretization of a piecewise linear approximation of the curve/surface. The analytical approximation therefore inherits the properties of the morphological discretization even when it is not equal to the morphological discretization.

Keywords: discretization, explicit curve/surface, morphological discretization, analytical approximation

MSC: 52C99

1 introduction

A curve or surface is continuous in the real world, while in the computer it is discretized to be stored and manipulated. It is therefore important to know how a discretized curve or surface is represented, where the representation differs depending on the employed discretization method. In the computer, the 2D plane is usually represented by a set of pixels, where each pixel is identified by its center coordinates; see Fig. 1(a). The 2D discrete space is therefore identified as $\mathbb{Z}^2$.

The discretization most commonly used is the *morphological discretization*[1] [13–15]. The discretized shape of a continuous curve or surface is there defined as a set of the integer points, whose Minkowski additions with a so-called *structuring element* intersect with the original shape. For example, the morphological discretization of a 2D curve using the unit square as a structuring element is given as the set of red pixels in Fig. 1(b). Some structuring elements are known to preserve topological properties of an original object [7–11, 19, 26–28].

How to discretize a curve or surface and how to compute the discretized curve or surface are different issues. Representing a discretized object (such as curve or surface) by the set of integer solutions of a system of inequalities, called the analytical representation, has been studied [1–6, 12, 21, 27, 28]. For some curves and surfaces, the morphological discretization (with some specific structuring elements) is known to have its analytical representation [2, 5, 6, 27, 28]. With the analytical representation, the morphological discretization is straightforwardly computed, just by evaluating inequalities for each integer point. This property is useful

***Corresponding Author: Fumiki Sekiya:** Dept. of Informatics, SOKENDAI (The Graduate University for Advanced Studies), Tokyo, Japan, E-mail: sekiya@nii.ac.jp
Akihiro Sugimoto: National Institute of Informatics, Tokyo, Japan, E-mail: sugimoto@nii.ac.jp

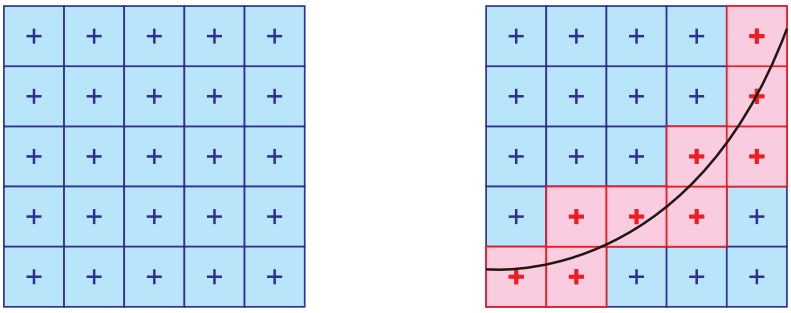

(a) 2D discrete space. (b) Discretization of a curve.

Figure 1: 2D discrete space and curve discretization.

also for fitting problems [17, 18, 20, 22, 24, 29, 30]. For complicated curves and surfaces, however, solving the corresponding inequality system is computationally expensive. To reduce the computational cost, an approximation of the analytical representation of the morphological discretization was introduced [27], where a discretized curve or surface is represented by a system of inequalities corresponding only to a finite subset of the employed structuring element. We call this the *analytical approximation*. In [27], the authors employed as a structuring element the *α-adjacency flake* ($\alpha = 0, \ldots, d-1$, where d is the dimension of the space) of radius $\frac{1}{2}$ and used only the end-points of the line segments composing the adjacency flake for the analytical approximation. They then proved that the discretization by the analytical approximation is equal to that by the morphological discretization if the boundary of the original curve or surface is *r-regular* [25] with $r > \frac{\sqrt{d-\alpha}+\sqrt{d}}{2}$. For curves and surfaces not satisfying this condition (e.g., those with a curvature radius smaller than $\frac{\sqrt{d-\alpha}+\sqrt{d}}{2}$), however, the discretization by the analytical approximation can be different from that by the morphological discretization. An example of such a curve in 2D is $y = 2x \sin(1/x)$ (if $x \neq 0$), 0 (otherwise) ($x, y \in \mathbb{R}$).

It is therefore significant to know the properties of the analytical approximation when it is not equal to the morphological discretization. In this paper, we study the properties of the analytical approximation focusing on discretization of continuous 2D explicit curves and 3D explicit surfaces, i.e., curves and surfaces in the form of $y = f(x)$ ($x, y \in \mathbb{R}$) and $z = f(x, y)$ ($x, y, z \in \mathbb{R}$). Such curves and surfaces are useful for representing an object by its contour or surface. We employ as our structuring element the *adjacency norm ball* [28] of radius $\frac{1}{2}$ and use only its vertices for the analytical approximation. We then show that the discretization of any continuous explicit curve or surface can be seen as the morphological discretization of a piecewise linear approximation of the curve or surface. This means that the analytical approximation inherits the properties of the morphological discretization even when it is not equal to the morphological discretization. We remark that the vertices of the adjacency norm ball are identical with the end-points of the line segments composing the adjacency flake, and therefore the analytical approximation in this paper is equivalent with that in [27]. We also remark that a part of this work has been reported [23].

2 Morphological discretization and analytical approximation

In this section, we first review the morphological discretization of continuous 2D explicit curves and 3D explicit surfaces, where we employ as a structuring element the α-adjacency norm ball [28] of radius $\frac{1}{2}$. We then give their analytical approximation based on the approach introduced in [27].

Let E_2 be a continuous 2D explicit curve, and E_3 be a continuous 3D explicit surface, namely,

$$\begin{aligned} E_2 &= \left\{(x, y) \in \mathbb{R}^2 \,\middle|\, y = f(x)\right\}, \\ E_3 &= \left\{(x, y, z) \in \mathbb{R}^3 \,\middle|\, z = g(x, y)\right\}, \end{aligned} \tag{1}$$

where $f : \mathbb{R} \to \mathbb{R}$ and $g : \mathbb{R}^2 \to \mathbb{R}$ are continuous functions.

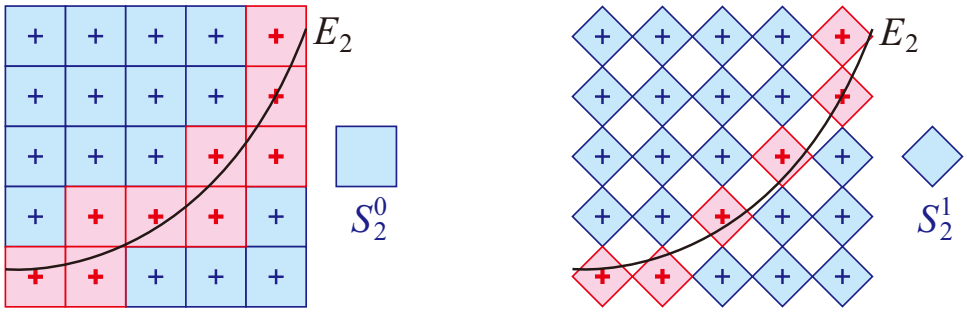

(a) $S = S_2^0$. (b) $S = S_2^1$.

Figure 2: Morphological discretizations $D_S(E_2)$ with $S = S_2^0, S_2^1$ (see Eq. (3)). Grid points depict the integer points, where the red ones are in $D_S(E_2)$.

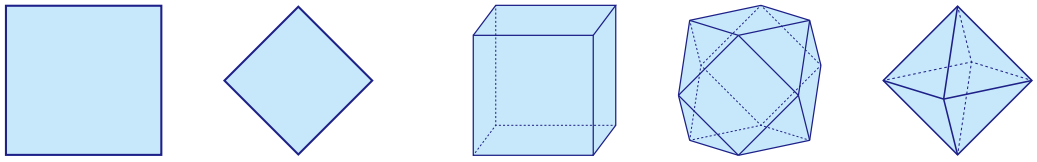

(a) S_2^0. (b) S_2^1. (c) S_3^0. (d) S_3^1. (e) S_3^2.

Figure 3: S_d^α for $d = 2, 3$ and $\alpha = 0, \ldots, d-1$.

2.1 Morphological discretization

The *morphological discretization* [14, 15] of E_d ($d = 2, 3$), with a *structuring element* $S \subset \mathbb{R}^d$, is defined by

$$D_S(E_d) = \left\{ \boldsymbol{v} \in \mathbb{Z}^d \,\middle|\, (\{\boldsymbol{v}\} \oplus S) \cap E_d \neq \emptyset \right\}, \tag{2}$$

where $\oplus$ denotes the Minkowski addition ($A \oplus B = \{\boldsymbol{a} + \boldsymbol{b} : \boldsymbol{a} \in A, \boldsymbol{b} \in B\}$). Figure 2 illustrates $D_S(E_d)$ for $d = 2$.

Using different structuring elements results in different discretizations (see Fig. 2 for example). How to select an appropriate structuring element is therefore an important issue. In this paper, we focus on structuring elements S_d^α ($d = 2, 3$ and $\alpha = 0, \ldots, d-1$) defined by

$$S_d^\alpha = \left\{ \boldsymbol{s} \in \mathbb{R}^d \,\middle|\, [\boldsymbol{s}]_\alpha \leq \frac{1}{2} \right\}, \tag{3}$$

where $[\cdot]_\alpha$ denotes the *α-adjacency norm* [28], i.e., for $\boldsymbol{s} \in \mathbb{R}^d$,

$$[\boldsymbol{s}]_\alpha = \max \left\{ \|\boldsymbol{s}\|_\infty, \frac{\|\boldsymbol{s}\|_1}{d - \alpha} \right\}.$$

Figure 3 depicts S_d^α for $d = 2, 3$ and $\alpha = 0, \ldots, d-1$.

2.2 Analytical approximation

Computing $D_{S_d^\alpha}(E_d)$ requires evaluating for each $\boldsymbol{v} \in \mathbb{Z}^d$ whether or not $\{\boldsymbol{v}\} \oplus S_d^\alpha$ intersects with E_d, which is computationally expensive. Based on the approach introduced in [27], however, we can compute it approximately at low cost.

We first give the analytical approximation for $d = 2$. From Eqs. (1) and (2), $D_{S_2^\alpha}(E_2)$ is written as

$$D_{S_2^\alpha}(E_2) = \left\{ (i, j) \in \mathbb{Z}^2 \,\middle|\, \begin{array}{l} \text{there exists } (x, y) \in S_2^\alpha \text{ satisfying} \\ j + y = f(i + x) \end{array} \right\}. \tag{4}$$

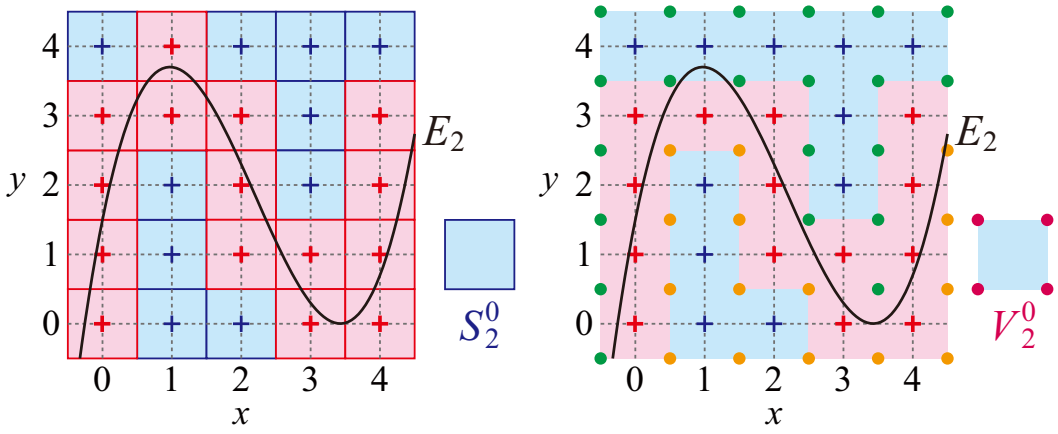

(a) $D_{S_2^0}(E_2)$. (b) $D_{V_2^0}(E_2)$.

Figure 4: $D_{S_2^0}(E_2)$ and $D_{V_2^0}(E_2)$ (red integer points) for $E_2 = \{(x, y) \in \mathbb{R}^2 \mid y = f(x) = 0.5x^3 - 3.3x^2 + 5x + 1.5\}$. In (b), points $(x, y) \in \mathbb{Z}^2 \oplus V_2^0$ satisfying $y > f(x)$ are depicted in green, while those satisfying $y < f(x)$ in orange; an integer point $\boldsymbol{v} \in \mathbb{Z}^2$ is in $D_{V_2^0}(E_2)$ iff $\{\boldsymbol{v}\} \oplus V_2^0$ (four points) are depicted in both colors, or include a point on E_2.

Note that $j + y = f(i + x)$ for $\exists(x, y) \in S_2^\alpha$ in Eq. (4) means $(\{(i, j)\} \oplus S_2^\alpha) \cap E_2 \neq \emptyset$. Since f is continuous and S_2^α is connected, the intermediate-value theorem allows us to rewrite Eq. (4) as

$$D_{S_2^\alpha}(E_2) = \left\{ (i, j) \in \mathbb{Z}^2 \;\middle|\; \begin{array}{c} \min\limits_{(x,y)\in S_2^\alpha} [f(i + x) - y] \\ \leq j \leq \\ \max\limits_{(x,y)\in S_2^\alpha} [f(i + x) - y] \end{array} \right\}. \tag{5}$$

Since S_2^α has infinite elements, unfortunately, evaluating the minimum and maximum of $f(i + x) - y$ with respect to $(x, y) \in S_2^\alpha$ is practically difficult. Following [27], the *analytical approximation* $D_{V_2^\alpha}(E_2)$ for $D_{S_2^\alpha}(E_2)$ is obtained by replacing S_2^α in Eq. (5) with V_2^α:

$$V_2^0 = \left\{ \left(-\tfrac{1}{2}, -\tfrac{1}{2}\right), \left(-\tfrac{1}{2}, \tfrac{1}{2}\right), \left(\tfrac{1}{2}, -\tfrac{1}{2}\right), \left(\tfrac{1}{2}, \tfrac{1}{2}\right) \right\},$$
$$V_2^1 = \left\{ \left(-\tfrac{1}{2}, 0\right), \left(0, -\tfrac{1}{2}\right), \left(0, \tfrac{1}{2}\right), \left(\tfrac{1}{2}, 0\right) \right\},$$

i.e., the vertices of S_2^α. Figure 4 illustrates the difference between the morphological discretization and its analytical approximation. Note that $D_{V_2^\alpha}(E_2) \subseteq D_{S_2^\alpha}(E_2)$ since $V_2^\alpha \subseteq S_2^\alpha$.

For $d = 3$, similarly to the 2D case, $D_{S_3^\alpha}(E_3)$ is first rewritten as

$$D_{S_3^\alpha}(E_3) = \left\{ (i, j, k) \in \mathbb{Z}^3 \;\middle|\; \begin{array}{c} \min\limits_{(x,y,z)\in S_3^\alpha} [g(i + x, j + y) - z] \\ \leq k \leq \\ \max\limits_{(x,y,z)\in S_3^\alpha} [g(i + x, j + y) - z] \end{array} \right\}. \tag{6}$$

The *analytical approximation* $D_{V_3^\alpha}(E_3)$ for $D_{S_3^\alpha}(E_3)$ is then obtained by replacing S_3^α in Eq. (6) with its vertices V_3^α:

$$V_3^\alpha = \left\{ (x, y, z) \;\middle|\; x, y, z \in \left\{-\tfrac{1}{2}, 0, \tfrac{1}{2}\right\} \text{ and } \|(x, y, z)\|_1 = \tfrac{3-\alpha}{2} \right\}.$$

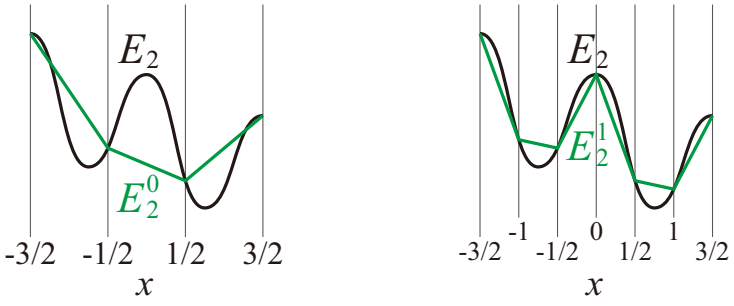

(a) $\alpha = 0$. (b) $\alpha = 1$.

Figure 5: Piecewise linear approximation E_2^α ($\alpha = 0, 1$) of E_2 for which $D_{V_2^\alpha}(E_2) = D_{S_2^\alpha}\left(E_2^\alpha\right)$.

3 Properties of morphological discretization preserved by analytical approximation

Now we show that the analytical approximation can be seen as the morphological discretization of a piecewise linear approximation of the original curve or surface, and therefore inherits the properties of the morphological discretization. Let $\mathbb{E}_d$ ($d = 2, 3$) denote the set of all E_d.

Theorem 1 *For any E_d with $d = 2, 3$ and $\alpha = 0, \ldots, d-1$, there exists $E_d^\alpha \in \mathbb{E}_d$ satisfying $D_{V_d^\alpha}(E_d) = D_{S_d^\alpha}\left(E_d^\alpha\right)$.*

Proof. We first consider the case of $d = 2$. For each $\alpha \in \{0, 1\}$, we give a continuous function $f^\alpha : \mathbb{R} \to \mathbb{R}$ such that $E_2^\alpha = \left\{(x, y) \in \mathbb{R}^2 \,\middle|\, y = f^\alpha(x)\right\}$ satisfies $D_{V_2^\alpha}(E_2) = D_{S_2^\alpha}\left(E_2^\alpha\right)$.

First, f^0 is defined as a piecewise linear approximation of f (the function determining E_2), which is uniquely determined as, for $\forall i \in \mathbb{Z}$, $f^0\left(i + \frac{1}{2}\right) = f\left(i + \frac{1}{2}\right)$, and $f^0(x)$ is linear for $x \in \left[i - \frac{1}{2}, i + \frac{1}{2}\right]$. Figure 5(a) shows E_2^0 determined by this f^0.

On the other hand, f^1 is defined as another piecewise linear approximation of f, which is uniquely determined as, for $\forall i \in \mathbb{Z}$, $f^1\left(\frac{i}{2}\right) = f\left(\frac{i}{2}\right)$, and $f^1(x)$ is linear for $x \in \left[\frac{i}{2}, \frac{i+1}{2}\right]$. Figure 5(b) shows E_2^1 determined by this f^1.

It is proven in essentially the same fashion for all $\alpha \in \{0, 1\}$ that f^α defined above satisfies $D_{V_2^\alpha}(E_2) = D_{S_2^\alpha}\left(E_2^\alpha\right)$. We therefore give the proof only for $\alpha = 1$. We transform $D_{S_2^1}\left(E_2^1\right)$ in the form of Eq. (5) into $D_{V_2^1}(E_2)$. Since $-\frac{1}{2} + |x| \le y \le \frac{1}{2} - |x|$ for $(x, y) \in S_2^1$, $D_{S_2^1}\left(E_2^1\right)$ is rewritten as

$$D_{S_2^1}(E_1^2) = \left\{ (i, j) \in \mathbb{Z}^2 \;\middle|\; \min_{x \in \left[-\frac{1}{2}, \frac{1}{2}\right]} \left[f^1(i + x) - \frac{1}{2} + |x| \right] \le j \le \max_{x \in \left[-\frac{1}{2}, \frac{1}{2}\right]} \left[f^1(i + x) + \frac{1}{2} - |x| \right] \right\}.$$

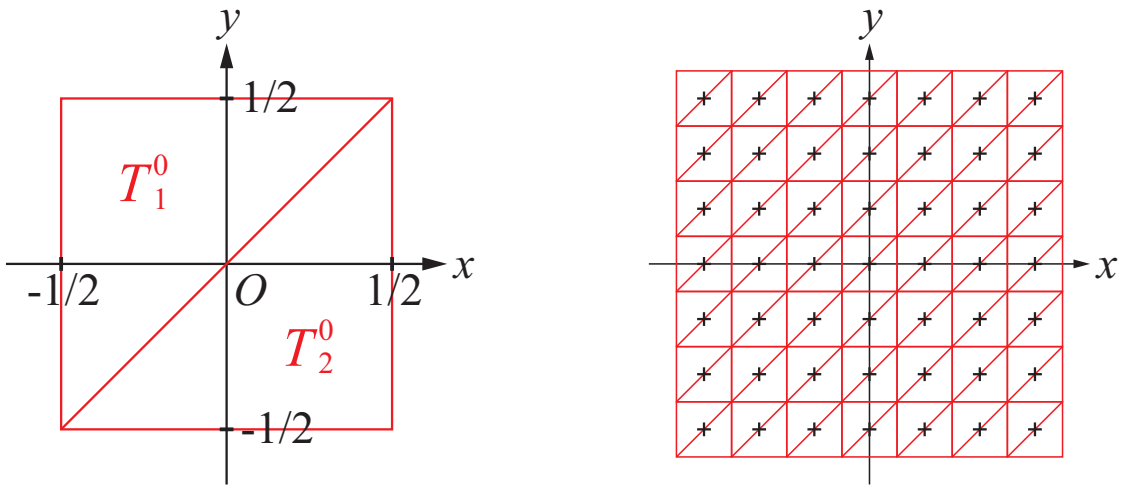

(a) T_1^0 and T_2^0. (b) Triangulation for E_3^0.

Figure 6: Triangulation of $\mathbb{R}^2$ based on which the piecewise linear approximation E_3^0 of E is defined to have $D_{V_3^0}(E_3) = D_{S_3^0}(E_3^0)$. The triangulation is constructed in terms of two triangles T_1^0 and T_2^0 in (a). In (b), black grid points depict integer points.

The minimum of $f^1(i+x) - \frac{1}{2} + |x|$ and the maximum of $f^1(i+x) + \frac{1}{2} - |x|$ with respect to $x \in \left[-\frac{1}{2}, \frac{1}{2}\right]$ are achieved at $x \in \left\{-\frac{1}{2}, 0, \frac{1}{2}\right\}$, since they are linear for $x \in \left[-\frac{1}{2}, 0\right]$ and $x \in \left[0, \frac{1}{2}\right]$. We therefore obtain

$$D_{S_2^1}(E_1^2) = \left\{ (i,j) \in \mathbb{Z}^2 \;\middle|\; \begin{array}{c} \min\left\{ \begin{array}{l} f^1\left(i-\frac{1}{2}\right), \\ f^1\left(i+\frac{1}{2}\right), \\ f^1(i) - \frac{1}{2} \end{array} \right\} \\ \leq j \leq \\ \max\left\{ \begin{array}{l} f^1\left(i-\frac{1}{2}\right), \\ f^1\left(i+\frac{1}{2}\right), \\ f^1(i) + \frac{1}{2} \end{array} \right\} \end{array} \right\},$$

in which we can replace f^1 by the original f since $f^1\left(\frac{i}{2}\right) = f\left(\frac{i}{2}\right)$ for $\forall i \in \mathbb{Z}$. We have $D_{S_2^1}(E_2^1) = D_{V_2^1}(E_2)$, consequently.

We next consider the case of $d = 3$. Similarly to the $d = 2$ case, we give a continuous function $g^\alpha : \mathbb{R}^2 \to \mathbb{R}$ ($\alpha \in \{0, 1, 2\}$) such that $E_3^\alpha = \left\{(x, y, z) \in \mathbb{R}^3 \;\middle|\; z = g^\alpha(x, y)\right\}$ satisfies $D_{V_3^\alpha}(E_3) = D_{S_3^\alpha}(E_3^\alpha)$.

First, g^0 is defined as a piecewise linear approximation of g (the function determining E_3), i.e., a triangle mesh surface, which is uniquely determined as, for $\forall (i,j) \in \mathbb{Z}^2$, $g^0\left(i+\frac{1}{2}, j+\frac{1}{2}\right) = g\left(i+\frac{1}{2}, j+\frac{1}{2}\right)$, and $g^0(x,y)$ is linear with respect to $(x,y) \in \{(i,j)\} \oplus T_n^0$ ($n = 1, 2$), where

$$T_1^0 = \left\{(x,y) \in \mathbb{R}^2 \;\middle|\; -\tfrac{1}{2} \leq x \leq y \leq \tfrac{1}{2}\right\},$$
$$T_2^0 = \left\{(x,y) \in \mathbb{R}^2 \;\middle|\; -\tfrac{1}{2} \leq y \leq x \leq \tfrac{1}{2}\right\}.$$

Figure 6(a) shows T_1^0 and T_2^0. We remark that g^0 has the same value with g on each vertex of the red triangles in Fig. 6(b), and it is locally linear within any of these triangles.

Next, g^1 is defined as another piecewise linear approximation of g, which is uniquely determined as follows: for $\forall (i,j) \in \mathbb{Z}^2$,

$$\begin{aligned} g^1\left(i, j+\tfrac{1}{2}\right) &= g\left(i, j+\tfrac{1}{2}\right), \\ g^1\left(i+\tfrac{1}{2}, j\right) &= g\left(i+\tfrac{1}{2}, j\right), \\ g^1\left(i+\tfrac{1}{2}, j+\tfrac{1}{2}\right) &= g\left(i+\tfrac{1}{2}, j+\tfrac{1}{2}\right), \end{aligned} \tag{7}$$

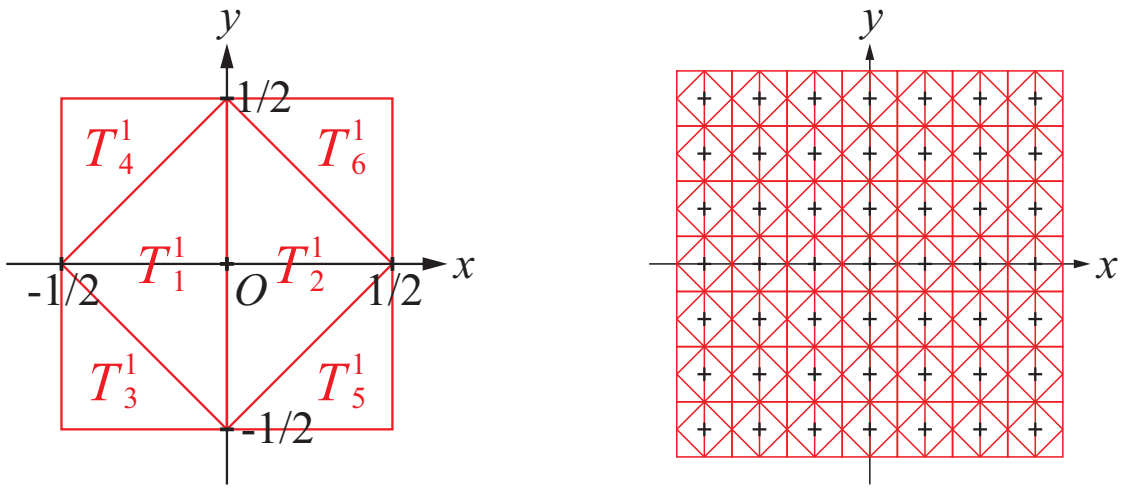

(a) $T_1^1, \ldots, T_6^1$. (b) Triangulation for E_3^1.

Figure 7: Triangulation of $\mathbb{R}^2$ based on which the piecewise linear approximation E_3^1 of E is defined to have $D_{V_3^1}(E_3) = D_{S_3^1}(E_3^1)$. The triangulation is constructed in terms of six triangles $T_1^1, \ldots, T_6^1$ in (a). In (b), black grid points depict integer points.

and $g^1(x, y)$ is linear with respect to $(x, y) \in \{(i, j)\} \oplus T_n^1$ $(n = 1, \ldots, 6)$, where

$$
\begin{aligned}
T_1^1 &= \left\{(x, y) \in \mathbb{R}^2 \,\middle|\, |x| + |y| \le \tfrac{1}{2},\ x \le 0\right\},\\
T_2^1 &= \left\{(x, y) \in \mathbb{R}^2 \,\middle|\, |x| + |y| \le \tfrac{1}{2},\ x \ge 0\right\},\\
T_3^1 &= \left\{(x, y) \in \mathbb{R}^2 \,\middle|\, |x| + |y| \ge \tfrac{1}{2},\ -\tfrac{1}{2} \le x \le 0,\ -\tfrac{1}{2} \le y \le 0\right\},\\
T_4^1 &= \left\{(x, y) \in \mathbb{R}^2 \,\middle|\, |x| + |y| \ge \tfrac{1}{2},\ -\tfrac{1}{2} \le x \le 0,\ 0 \le y \le \tfrac{1}{2}\right\},\\
T_5^1 &= \left\{(x, y) \in \mathbb{R}^2 \,\middle|\, |x| + |y| \ge \tfrac{1}{2},\ 0 \le x \le \tfrac{1}{2},\ -\tfrac{1}{2} \le y \le 0\right\},\\
T_6^1 &= \left\{(x, y) \in \mathbb{R}^2 \,\middle|\, |x| + |y| \ge \tfrac{1}{2},\ 0 \le x \le \tfrac{1}{2},\ 0 \le y \le \tfrac{1}{2}\right\}.
\end{aligned}
$$

Fig. 7(a) shows $T_1^1, \ldots, T_6^1$. We remark that g^1 has the same value with g on each vertex of the red triangles in Fig. 7(b), and it is locally linear within any of these triangles.

Finally, g^2 is defined as yet another piecewise linear approximation of g, which is uniquely determined as, for $\forall (i, j) \in \mathbb{Z}^2$, $g^2\left(\frac{i}{2}, \frac{j}{2}\right) = g\left(\frac{i}{2}, \frac{j}{2}\right)$, and $g^2(x, y)$ is linear with respect to $(x, y) \in \{(i, j)\} \oplus T_n^2$ for $n = 1, \ldots, 6$, where

$$
\begin{aligned}
T_1^2 &= \left\{(x, y) \in \mathbb{R}^2 \,\middle|\, |x| + |y| \le \tfrac{1}{2},\ x \le 0,\ y \le 0\right\},\\
T_2^2 &= \left\{(x, y) \in \mathbb{R}^2 \,\middle|\, |x| + |y| \le \tfrac{1}{2},\ x \le 0,\ y \ge 0\right\},\\
T_3^2 &= \left\{(x, y) \in \mathbb{R}^2 \,\middle|\, |x| + |y| \le \tfrac{1}{2},\ x \ge 0,\ y \le 0\right\},\\
T_4^2 &= \left\{(x, y) \in \mathbb{R}^2 \,\middle|\, |x| + |y| \le \tfrac{1}{2},\ x \ge 0,\ y \ge 0\right\},\\
T_5^2 &= \left\{(x, y) \in \mathbb{R}^2 \,\middle|\, -\tfrac{1}{2} \le x \le 0,\ x \le y - \tfrac{1}{2} \le -x\right\},\\
T_6^2 &= \left\{(x, y) \in \mathbb{R}^2 \,\middle|\, 0 \le x \le \tfrac{1}{2},\ -x \le y - \tfrac{1}{2} \le x\right\}.
\end{aligned}
$$

Figure 8(a) shows $T_1^2, \ldots, T_6^2$. We remark that g^2 has the same value with g on each vertex of the red triangles in Fig. 8(b), and it is locally linear within any of these triangles.

It is proven in essentially the same fashion for all $\alpha \in \{0, 1, 2\}$ that g^α defined above satisfies $D_{V_3^\alpha}(E_3) = D_{S_3^\alpha}(E_3^\alpha)$. We therefore give the proof only for $\alpha = 1$. We transform $D_{S_3^1}(E_3^1)$ in the form of Eq. (6) into $D_{V_3^1}(E_3)$. For $(x, y, z) \in S_3^1$, z is related to x and y as $-h(x, y) \le z \le h(x, y)$ where

$$
h(x, y) = \begin{cases} \frac{1}{2} & \text{if } |x| + |y| \le \frac{1}{2} \\ 1 - |x| - |y| & \text{if } |x| + |y| > \frac{1}{2} \end{cases}.
$$

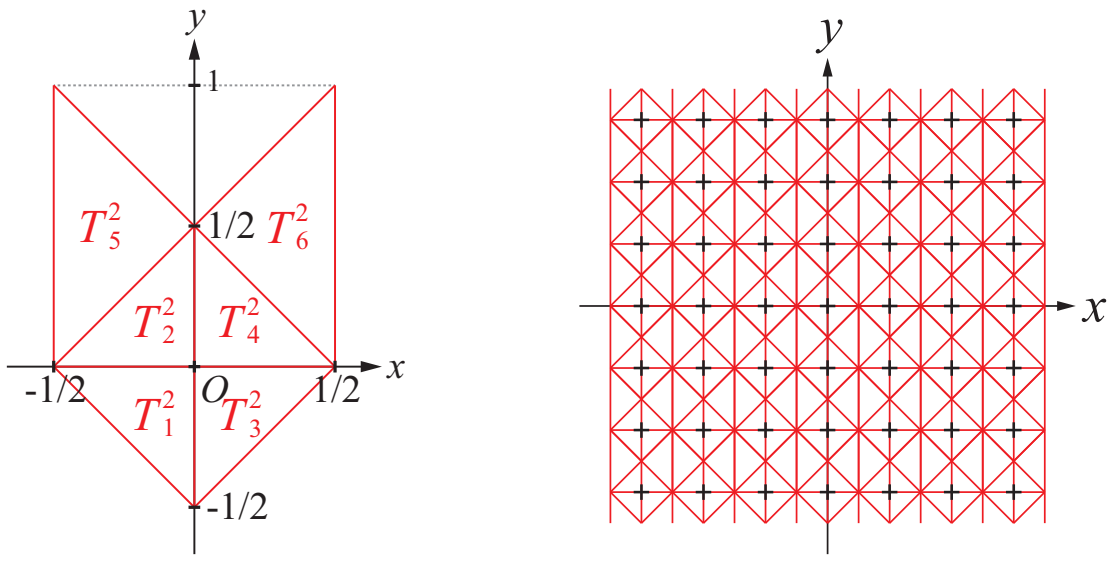

(a) $T_1^2, \ldots, T_6^2$. (b) Triangulation for E_3^2.

Figure 8: Triangulation of $\mathbb{R}^2$ based on which the piecewise linear approximation E_3^2 of E is defined to have $D_{V_3^2}(E_3) = D_{S_3^2}(E_3^2)$. The triangulation is constructed in terms of six triangles $T_1^2, \ldots, T_6^2$ in (a). In (b), black grid points depict integer points.

Note that $|x|, |y| \le \frac{1}{2}$. $D_{S_3^1}(E_3^1)$ is therefore written as

$$D_{S_3^1}(E_3^1) = \left\{ \begin{array}{c|c} (i,j,k) & \min\limits_{|x|,|y|\le\frac{1}{2}} \left[g^1(i+x, j+y) - h(x,y) \right] \\ \in \mathbb{Z}^3 & \le k \le \\ & \max\limits_{|x|,|y|\le\frac{1}{2}} \left[g^1(i+x, j+y) + h(x,y) \right] \end{array} \right\}.$$

$|x|, |y| \le \frac{1}{2}$ is equivalent to $(x,y) \in \bigcup_{n=1}^{6} T_n^1$. For $(i,j) \in \mathbb{Z}^2$, furthermore, both $g^1(i+x, j+y)$ and $h(x,y)$ are linear with respect to $(x,y) \in T_n^1$ for $n = 1, \ldots, 6$. The extrema of $g^1(i+x, j+y) \pm h(x,y)$ are therefore obtained at $(x,y) \in \left\{ \left(\pm\frac{1}{2}, 0\right), \left(0, \pm\frac{1}{2}\right), \left(\pm\frac{1}{2}, \pm\frac{1}{2}\right) \right\}$ (the vertices of the triangles), where $\left(\pm\frac{1}{2}, 0\right)$ counts $\left(-\frac{1}{2}, 0\right)$ and $\left(\frac{1}{2}, 0\right)$, and similarly for the other elements. We thus obtain

$$D_{S_3^1}(E_3^1) = \left\{ \begin{array}{c|c} (i,j,k) \in \mathbb{Z}^3 & \min \left\{ \begin{array}{l} g^1\left(i \pm \frac{1}{2}, j \pm \frac{1}{2}\right), \\ g^1\left(i \pm \frac{1}{2}, j\right) - \frac{1}{2}, \\ g^1\left(i, j \pm \frac{1}{2}\right) - \frac{1}{2} \end{array} \right\} \\ & \le k \le \\ & \max \left\{ \begin{array}{l} g^1\left(i \pm \frac{1}{2}, j \pm \frac{1}{2}\right), \\ g^1\left(i \pm \frac{1}{2}, j\right) + \frac{1}{2}, \\ g^1\left(i, j \pm \frac{1}{2}\right) + \frac{1}{2} \end{array} \right\} \end{array} \right\},$$

in which g^1 can be replaced by the original g from Eq. (7). We have $D_{S_3^1}(E_3^1) = D_{V_3^1}(E_3)$, consequently. □

4 Concluding remarks

We studied the properties of the morphological discretization preserved by the analytical approximation, focusing on discretization of continuous 2D explicit curves and 3D explicit surfaces. We employed as our

structuring element the α-adjacency norm ball of radius $\frac{1}{2}$ and used only its vertices for the analytical approximation. We showed that the discretization of any continuous explicit curve or surface by the analytical approximation can be seen as the morphological discretization of a piecewise linear approximation of the curve or surface (Theorem 1). This means that, for continuous explicit curves and surfaces, any discussion in the literature about the properties of the morphological discretization can be applied to the analytical approximation. For example, the property that the morphological discretization with the 0-adjacency norm ball of radius $\frac{1}{2}$ preserves the connectivity [8] and the separability [11] of an original object, is inherited to the analytical approximation, i.e., $D_{V_2^0}(E_2)$ is 4-connected and 8-separating for any $E_2 \in \mathbb{E}_2$, and $D_{V_3^0}(E_3)$ is 6-connected and 26-separating for any $E_3 \in \mathbb{E}_3$. Such properties of the analytical approximation can be also derived from the morphological discretization using the α-adjacency flake of radius $\frac{1}{2}$. This is because Theorem 1 holds true also in the case where the structuring element is the α-adjacency flake of radius $\frac{1}{2}$. For $d = 2, 3$ and $\alpha = 0, \ldots, d-1$, the piecewise linear approximation in the proof of Theorem 1 has been designed so that the extrema in the inequalities determining the morphological discretization are always achieved by vertices of the α-adjacency norm ball. Since the α-adjacency flake is a subset of the α-adjacency norm ball (the vertices are identical with the end-points of the line segments composing the α-adjacency flake), those extrema remain the same even if the structuring element is replaced with the α-adjacency flake. The α-adjacency flake thus yields the same morphological discretization as the α-adjacency norm ball for the piecewise linear approximation, which is equal to the analytical approximation.

This work might be extended to more general 2D curves and 3D surfaces in the form of $f(x, y) = 0$ and $f(x, y, z) = 0$. This is because they can be split into pieces, each of which is represented in the form of $y = f(x)$ and $z = f(x, y)$ where the domain of each function is bounded (not $\mathbb{R}$ or $\mathbb{R}^2$ as discussed in this paper). This extension is however not straightforward because the analytical approximation cannot be directly applied to a function whose domain is bounded. At the ends (2D) or edges (3D) of a (split piece) function, a point may arise for which we cannot evaluate all the vertices in V_d^α. We thus cannot determine whether or not it should be involved in the discretization of the function. Simply excluding such points brings disconnection between the discretized pieces. Investigating this issue and addressing the extension to more general 2D curves and 3D surfaces are left for future work.

References

[1] Eric Andres. Discrete linear objects in dimension n: the standard model. *Graphical Models*, 65(1):92–111, 2003.

[2] Eric Andres. The supercover of an m-flat is a discrete analytical object. *Theoretical Computer Science*, 406(1):8–14, 2008.

[3] Eric Andres, Raj Acharya, and Claudio Sibata. Discrete analytical hyperplanes. *Graphical Models and Image Processing*, 59(5):302–309, 1997.

[4] Eric Andres and Marie-Andrée Jacob. The discrete analytical hyperspheres. *IEEE Transactions on Visualization and Computer Graphics*, 3(1):75–86, 1997.

[5] Eric Andres, Philippe Nehlig, and Jean Françon. Supercover of straight lines, planes and triangles. In *Discrete Geometry for Computer Imagery*, pages 243–254. Springer, 1997.

[6] Eric Andres and Tristan Roussillon. Analytical description of digital circles. In *Proc. of International Conference on Discrete Geometry for Computer Imagery (DGCI2011)*, volume 6607 of *LNCS*, pages 235–246. Springer, 2011.

[7] Valentin E Brimkov. On connectedness of discretized objects. In *Advances in Visual Computing*, pages 246–254. Springer, 2013.

[8] Valentin E Brimkov, Eric Andres, and Reneta P Barneva. Object discretization in higher dimensions. In *Proc. of International Conference on Discrete Geometry for Computer Imagery (DGCI2000)*, volume 1953 of *LNCS*, pages 210–221. Springer, 2000.

[9] Valentin E Brimkov, Reneta P Barneva, and Boris Brimkov. Minimal offsets that guarantee maximal or minimal connectivity of digital curves in nD. In *Proc. of International Conference on Discrete Geometry for Computer Imagery (DGCI2009)*, volume 5810 of *LNCS*, pages 337–349. Springer, 2009.

[10] Valentin E Brimkov, Reneta P Barneva, and Boris Brimkov. Connected distance-based rasterization of objects in arbitrary dimension. *Graphical Models*, 73(6):323–334, 2011.

[11] Daniel Cohen-Or and Arie Kaufman. Fundamentals of surface voxelization. *Graphical Models and Image Processing*, 57(6):453–461, 1995.

[12] Yan Gérard, Laurent Provot, and Fabien Feschet. Introduction to digital level layers. In *Proc. of the International Conference on Discrete Geometry for Computer Imagery (DGCI2011)*, volume 6607 of *LNCS*, pages 83–94. Springer-Verlag, 2011.

[13] Henk J A M Heijmans. Morphological discretization. *Geometrical Problems of Image Processing*, pages 99–106, 1991.
[14] Henk J A M Heijmans. Discretization of morphological operators. *Journal of Visual Communication and Image Representation*, 3(2):182–193, 1992.
[15] Henk J A M Heijmans and Alexander Toet. Morphological sampling. *CVGIP: Image Understanding*, 54(3):384–400, 1991.
[16] Reinhard Klette and Azriel Rosenfeld. *Digital geometry: geometric methods for digital picture analysis*. Elsevier, 2004.
[17] Gaelle Largeteau-Skapin, Rita Zrour, and Eric Andres. $O(n^3 \log n)$ time complexity for the optimal consensus set computation for 4-connected digital circles. In *Proc. of the International Conference on Discrete Geometry for Computer Imagery (DGCI2013)*, volume 7749 of *LNCS*, pages 241–252. Springer, 2013.
[18] Gaëlle Largeteau-Skapin, Rita Zrour, Eric Andres, Akihiro Sugimoto, and Yukiko Kenmochi. Optimal consensus set and preimage of 4-connected circles in a noisy environment. In *Proc. of the International Conference on Pattern Recognition (ICPR2012)*, pages 3774–3777. IEEE, 2012.
[19] Christoph Lincke and Charles A. Wüthrich. Surface digitizations by dilations which are tunnel-free. *Discrete Applied Mathematics*, 125(1):81–91, 2003.
[20] Minh Son Phan, Yukiko Kenmochi, Akihiro Sugimoto, Hugues Talbot, Eric Andres, and Rita Zrour. Efficient robust digital annulus fitting with bounded error. In *Proc. of the International Conference on Discrete Geometry for Computer Imagery (DGCI2013)*, volume 7749 of *LNCS*, pages 253–264. Springer, 2013.
[21] Jean-Pierre Reveillès. *Géométrie discrete, calcul en nombres entiers et algorithmique*. PhD thesis, Dèpartement d'Informatique, Université Louis Pasteur, Strasbourg, France, 1991.
[22] Fumiki Sekiya and Akihiro Sugimoto. Fitting discrete polynomial curve and surface to noisy data. *Annals of Mathematics and Artificial Intelligence*, 75(1-2):135–162, 2015.
[23] Fumiki Sekiya and Akihiro Sugimoto. On connectivity of discretized 2D explicit curve. In *Mathematical Progress in Expressive Image Synthesis II*, pages 33–44. Springer, 2015.
[24] Abdoulaye Sere, Oumarou Sie, and Emmanuel Andres. Extended standard Hough transform for analytical line recognition. In *Proc. of International Conference on Sciences of Electronics, Technologies of Information and Telecommunications (SETIT2012)*, pages 412–422. IEEE, 2012.
[25] Peer Stelldinger and Ullrich Köthe. Towards a general sampling theory for shape preservation. *Image and Vision Computing*, 23(2):237–248, 2005.
[26] Mohamed Tajine and Christian Ronse. Topological properties of Hausdorff discretization, and comparison to other discretization schemes. *Theoretical Computer Science*, 283(1):243–268, 2002.
[27] Jean-Luc Toutant, Eric Andres, Gaëlle Largeteau-Skapin, and Rita Zrour. Implicit digital surfaces in arbitrary dimensions. In *Proc. of the International Conference on Discrete Geometry for Computer Imagery (DGCI2014)*, volume 8668 of *LNCS*, pages 332–343. Springer, 2014.
[28] Jean-Luc Toutant, Eric Andres, and Tristan Roussillon. Digital circles, spheres and hyperspheres: From morphological models to analytical characterizations and topological properties. *Discrete Applied Mathematics*, 161(16):2662–2677, 2013.
[29] Rita Zrour, Yukiko Kenmochi, Hugues Talbot, Lilian Buzer, Yskandar Hamam, Ikuko Shimizu, and Akihiro Sugimoto. Optimal consensus set for digital line and plane fitting. *International Journal of Imaging Systems and Technology*, 21(1):45–57, 2011.
[30] Rita Zrour, Gaëlle Largeteau-Skapin, and Eric Andres. Optimal consensus set for annulus fitting. In *Proc. of the International Conference on Discrete Geometry for Computer Imagery (DGCI2011)*, volume 6607 of *LNCS*, pages 358–368. Springer, 2011.

Notes

[1] Some classical discretizations, such as the supercover discretization [11] or the grid-intersection discretization [16], can be seen as special cases of the morphological discretization.